This article has been published in the Journal of Materials Research. The final publication is available at Cambridge via https://doi.org/10.1557/jmr.2016.163 .

Alloy development and reheating process exploration of Al-Si casting alloys with globular grains for thixoforming

JiaoJiao Wang[a,*], ZhongMin Zhang [b], A.B. Phillion [c], ShuZhen Shang [a], GuiMin Lu [a,*]

[a] The Key Laboratory of Pressure Systems and Safety, Ministry of Education, East China University of Science and Technology, Shanghai, 200237, China

[b] Shanghai Junsoft Digital Science & Technology Co., Ltd, Shanghai, 200051, China

[c] Materials Science and Engineering, McMaster University, Hamilton, L8S 4L7, Canada

Abstract: A novel two-stage reheating process with new alloy design has been developed to improve the microstructure morphology of semi-solid Al-Si casting aluminum alloy for thixoforming. The process consists of first reheating the material to the liquidus temperature, holding for 5 minutes, and then lowering to the predetermined two-stage reheating temperature between 843 -863 K and holding for 10 minutes. The experimentally-obtained grain diameter, roundness, and the amount of liquid trapped within the solid phase were characterized, along with the microstructure obtained using the traditional feedstock reheating process. The Wilcox test (with α=0.05) was then applied to statistically analyze the measured differences in the microstructures obtained using the two different processing routes. It was found that a refined near-spherical structure with uniform globule size, higher sphericity, lower coarsening rate constant, and less entrapped liquid was obtained via the new two-stage reheating process in comparison with the microstructure obtained using the traditional feedstock reheating process.

Keywords: casting, morphology, microstructure

1. Introduction

Thixoforming is a near-net-shape manufacturing process that is performed at temperatures between the solidus and the liquidus [1-3], with different recrystallization behavior from conventional process [4-8]. The most distinct characteristic of thixoformed microstructure is the co-existence of liquid and solid during processing (since this occurs at semi-solid temperatures), and the formation of a primary phase with near-spherical grain morphology [9-11]. This process has received considerable attention recently due to its significant advantages over traditional metal forming process, such as minimization of as-cast porosity and macro-segregation; reduced forming temperatures, forming forces, and machining costs; and high strength and corrosion resistance [12-15].

During the thixoforming process, the billet feedstock is reheated into the semi-solid state before the forming operation. It is well known that semi-solid alloys have a thixotropic behavior in which the fluidity is time-dependent and strongly shear-thinning, meaning that at rest the material can be handled like a solid, and during shearing it becomes very fluid with liquid-like flow [16, 17]. This behavior greatly relies on non-dendritic and spherical/globular microstructure being achieved during the feedstock preparation process [1-3]. Tzimas and Zavaliangos [18] reported that the geometry of the solid grains plays an important role in

*Corresponding author. Tel.: +86 21 64252065; fax: +86 21 64252501.
E-mail address: jiaojiaowang.wendy@hotmail.com (J. J. Wang*), gmlu@ecust.edu.cn (G. M. Lu*)

determining the flow response of the material during thixoforming, while Meng et al. [19-21] showed that the mechanical behavior of a material during semi-solid forming is strongly affected by the morphology of the microstructure. Moradi et al. [22] also demonstrated that the finer and globular-shape particles obtained from reheating process is the major factor for the success of thixoforming. Thus, precise control of the reheating stage is very important, in order to create semi-solid material with a specified fraction solid, and with fine and uniform globular microstructure.

At present, although much of the new research and application of thixoforming is focused on wrought metallic alloy developments [23-25], most commercial thixoforming is performed using conventional aluminum-based casting alloys owing to their high fluidity and good 'castability'. Specifically, there is great interest in using Al-Si alloys as a material for thixoforming due to the fact that Al-Si alloys have a relatively wide solid-liquid temperature interval and high fluidity in the semi-solid region [26]. These properties help to achieve good quality thixoformed components. In this work, a novel two-stage reheating process, recently proposed by Wang et al. [27] for AA6061, is explored for application to Al-Si casting alloys. Please note that the idea of two-stage reheating process is the same as in AA6061, but the actual method used for wrought and casting alloys are different. The first-stage of the reheating process for wrought alloys is a reheat to the solidus temperature, while for casting aluminum alloys, the liquidus temperature is used as the starting point. Based on the conventional Al-Si casting alloy, 356.0, composition and process design were tailored to enable the development of a high-strength aluminum casting alloy with superior characteristics for thixoforming. The coarsening rate constant, fraction of entrapped liquid, grain size and shape are evaluated under various processing conditions and reported for both the two-stage and the traditional feedstock reheating processes in order to compare the differences in microstructure obtained using each method.

2. Experimental procedures

2.1. Alloy development

The material investigated in this work was a variant of the common commercial 356.0 Al-Si casting alloy, with a chemical composition as given in Table 1. This new alloy, denoted 356.0v has a lower Si content (6.01 vs. 6.5-7.5 wt. %) and a higher Mg content (0.52 vs. 0.20-0.45, wt. %) as compared to 356.0, and was developed specifically for thixoforming. Except for Si and Mg, the chemical composition of 356.0v falls within the standard range found in the ASM Handbook [28]. The modification of the Si and Mg was developed to improve thixoformability of casting Al-Si casting alloys whilst also approaching the performance of wrought alloys. The specific content of Si and Mg in 356.0v were determined according to the thermodynamic and phase equilibriums method [29]. First of all, a slight decrease in Si content was applied to enlarge the solidus-liquidus interval, in order to facilitate semi-solid processing. The additional Mg was added to assist in forming additional Mg_2Si, which will improve the macroscopic mechanical properties. Further, additional Mg will result in a primary-phase grain refinement [30]. Salleh et al. [31] indicated that the fracture behavior of the thixoformed alloys was improved after a T6 heat treatment, with significantly higher ductility.

Table 1 Chemical compositions (wt. %) of 356.0 alloy in ASM Handbook and developed

356.0v alloy measured with a PMI-MASTER PRO.

Alloy	Si	Mg	Fe	Mn	Ti	Cu	Zn	Cr	Al
356.0	6.5-7.5	0.20-0.45	0.6	0.35	0.25	0.25	0.35	0.5	Bal.
356.0v	6.01	0.52	0.21	0.20	0.17	0.088	0.029	0.02	Bal.

The initial microstructure of the developed 356.0v alloy, obtained from vertical electromagnetic continuous casting billets 70 mm in diameter, is shown in Fig. 1. As can be seen, this microstructure consists of fine dendritic grains with a few bright phases of blocky Si precipitates distributed at the grain boundaries. This blocky Si phase will re-melt once the material heated to a temperature above the eutectic point. Assuming that thixoforming eliminates the blocky Si, these precipitate will not cause embitterment [32] during usage. After casting, samples 15 ×15 ×15 mm^3 were machined from the billet for the reheating experiments.

2.2. Thermal analysis

The process of thixoforming requires a solidus-liquidus interval that is wide enough to facilitate the formation of spherical solid grain. According to the Al-Si phase diagram, a reduction in the Si content from 7 to 6 wt. % will increase the solidus-liquidus interval. To accurately determine the evolution in fraction solid with temperature for 356.0v, along with the solidus and liquidus temperatures, differential scanning calorimetry (DSC) was performed using a NETZSCH STA 449 F3 thermal analysis system. The heat flow signal obtained via DSC during cooling of a small sample is shown in Fig. 2. As can be seen, the solidus and liquidus temperatures of 356.0v are 812K and 914K, respectively. Thus, the solidus-liquidus temperature range for 356.0v is nearly 70% larger as compared to 356.0 (888K and 828K [28]). The corresponding evolution of liquid fraction calculated from the DSC heat flow data by integration is given in Fig. 3. As can be seen, the slope of the curve is quite high at temperatures above 840K because this alloy, like 356.0, contains a significant fraction of eutectic.

2.3 Two-stage reheating process

A Muffle Furnace (Fisher Scientific 550 -126) was used to reheat the sample to the semi-solid region during the reheating process, with an average heating rate of 10 K/min. As discussed in previous research [27], the advantage of using a two-stage reheating process when preparing feedstock for thixoforming is to create microstructure that has both a continuous solid skeleton for handling purposes and provides thixotropic behavior during thixoforming. Based on the results shown in Fig. 3, it is also noticed that the amount of eutectic represents the position of the ‘knee’ existing for fraction liquid vs. temperature curve. The existence of a knee at around liquid fraction of 0.5 gives controllability in the thixoforming process [29]. This knee of 356.0v casting alloy just locates around fraction liquid of 0.5, corresponding to the start of the non-equilibrium eutectic melting point. In effect, it acts as a ‘brake’ on the liquid formation, which make the 356.0v casting alloy is so suitable for thixoforming.

A comprehensive investigation was then undertaken to compare the microstructure obtained from both the traditional reheating process for thixoforming, and the proposed two-stage

method. For the traditional reheating process, the samples were directly reheated to 843, 853, and 863K in the muffle furnace, and then quenched after holding times of 15, 20, 25min. This corresponds to (see Fig. 3), liquid fractions of 0.1, 0.3 and 0.5, respectively. For the two-stage reheating process[b], the billets were first reheated to the liquidus temperature for 5 min (corresponding to stage 1), then cooled to 843, 853, and 863 K over a 5 min cooling period, and finally held at temperature for 5, 10 and 15 min, respectively (corresponding to stage 2). A schematic of the process route is depicted in Fig. 4. Please note that when the sample was reheated to liquidus temperature during the first stage, the semi-solid billets still held its own weigh thus its initial solid cubic shape could be maintained as a result of the reasonable controlling of holding temperature. All samples after reheating process were then rapidly quenched in cold water to freeze the semi-solid microstructures for optical microscopy. The quenched specimens were grounded, polished and then etched with the mixed acid solution of 2 ml HF, 3 ml HCl, 5 ml HNO_3, and 190 ml H_2O. The optical microstructures were observed by an inverted microscope, Axio Observer A1m.

2.4 Data Analysis

Optical micrographs of each specimen were obtained using an Axio Observer A1m. The resulting microstructures were then analyzed using image analysis methods. The grain diameter, roundness, and the amount of liquid trapped within the solid phase were evaluated using Image Pro Plus (IPP) analysis software. The average grain size and grain shape were described by equivalent diameter (D_{eq}) and roundness (F) of solid grains, which were respectively defined by following relationships [3].

$$D_{eq} = \frac{1}{n}\sum_{n=1}^{n}\sqrt{\frac{4A_n}{\pi}} \qquad (1)$$

$$F = \frac{1}{n}\sum_{n=1}^{n}\frac{4\pi A_n}{P_n^{\,2}} \qquad (2)$$

where A_n denotes the area of the solid grains, P_n is the perimeter of the solid grains and n is the number of the solid grains. In the case of perfectly spherical solid grain, the value of F is equal to 1. The amount of entrapped liquid is compared against the total amount of liquid, resulting in the term fraction of entrapped liquid, $f_{l,en}$. This term varies between 0 and 1. $f_{l,en} = 0$ corresponds to the case where there is no liquid droplets within the solid grains but instead all the liquid is free and at the grain boundaries. This situation is preferable, from a

[b] An initial study for casting aluminium alloy was carried out on six different heating routes near the solidus and the liquidus temperatures following [27] to determine the optimum intermediate time /temperature combination. Based on this initial study, the use of the liquidus as the intermediate temperature and a 5 min intermediate reheating time was optimal for promoting the desired microstructure for thixoforming.

quality perspective, since a high content of entrapped liquid may induce defects like shrinkage porosity during thixoforming. $f_{l,en}=1$ corresponds to the case where all the liquid is encapsulated within a solid grain.

The kinetics of grain coarsening were quantified using the Lifshitz–Slyozov–Wagner (LSW) theory, as follows [33],

$$D_{eq}^{\ 3} - D_{eq0}^{\ 3} = Kt \qquad (3)$$

where D_{eq} is equivalent diameter of solid grain at time *t*, and D_{eq0} at time $t=0$, *K* is the coarsening rate constant. The solid grain equivalent diameter measured at after a 15 min holding time was used as the value for D_{eq0}.

Statistical tests were then applied to the obtained quantified data in order to characterize the significance of the results. Specifically, the non-parameter Wilcox test (α=0.05) was applied, using the open-source *R* statistical package [34], to compare the data from the traditional and two-stage reheating processes[c] (D_{eq} and *F* from the solid grains, $f_{l,en}$ from the liquid, and *K*). As the measurement for each sample was taken from the whole micrograph, the sample size for each parameter of *F*, D_{eq}, $f_{l,en}$ were different. Sampling was conducted to evaluate the mean value of K, with the number of samples and sampling time set as 30 and 1000 s, respectively.

The Wilcox test is a measure of similarity. This test begins with the assumption that the mean values between two micrographs are equal to each other, *i.e.* $x_1=x_2$, known as the null hypothesis. The output of the Wilcox test is a p-value. If $p<0.05$, then the null hypothesis is refused, *i.e.* $x_1 \neq x_2$. Otherwise, the null hypothesis is accepted.

In order to validate the use of image analysis methods, and meanwhile to reduce the amount of manual interventions, one of the grain shape parameters, the prediction of average grain roundness made by the IPP software (denoted *F**) and Eq. (2) (denoted *F*) were compared. The Wilcox test results are given in Table 2. As can be seen, the p-value of (*F**&*F*) for a given reheating process is quite high, nearly 1. Since $p>0.05$, there is no significant difference in the mean value of roundness predicted by IPP (*F**) and Eq. 2 (*F*). Therefore, the measured results of area (A_n) and perimeter (P_n) of solid grains obtained from software IPP are reliable, which can be reasonably substituted in Eq. (1) ~ (3) for the quantitative investigation on the semi-solid microstructure evolution of casting aluminum alloy.

Table 2 The p-values from the Wilcox tests (α=0.05) for the parameter of roundness of solid grains measured results from IPP and the mathematic theoretical results by using Equation (2)

[c] The non-parameter Wilcox test was selected as the statistical algorithm because, based on the Shapiro test, the microstructure morphology data was not normally distributed.

at the same experimental condition.

Reheating parameters	843K, 15min	843K, 20min	843K, 25min	853K, 15min	853K, 20min	853K, 25min	863K, 15min	863K, 20min	863K, 25min
p-value of *F**& *F*	0.9362	0.9022	0.9026	0.9222	0.9101	0.9017	0.9189	0.9232	0.9312

3. Results and discussion

3.1 Qualitative comparison between traditional and two-stage processes

Figs. 5, 6, and 7 show a comparison between the traditional and two-stage reheating processes to prepare feedstock for thixoforming. Each figure provides the microstructures resulting from using a different reheating temperature (843, 853, and 863 K), and within each figure the reheating time is increased from top to bottom (15, 20, and 25 min). The micrographs on the left (right) were taken from samples processed using the traditional (two-stage) reheating process. Overall, it can be seen from this series of micrographs that solid grains coarsen gradually with increased temperatures and holding times, through two main mechanisms of coalescence and Ostwald ripening. Coalescence occurs by boundary migration when two adjacent grains with similar size share a common crystallographic orientation [2], as indicated by two-way arrow in Figs.5-7. Large coalescence resulted from small solid grains merge into larger ones to reduce the interfacial energy was noticed in the semi-solid microstructure (marked as ‘C’ in Figs. 5-7). Ostwald ripening was also observed to occur, with large grains growing at the expense of small ones, as indicated by one-way arrow in Figs. 5-7. Active small grains with larger surface area to volume ratio will attain a lower energy state by transforming into large grains. Another form of coalescence that was observed in the micrographs is the agglomeration of two or more small neighbor grains (marked as ‘O’ in Figs. 5-7). These were likely to have some small liquid droplets appeared inside of solid grains or its agglomeration, labeled as ‘I’ in Figs. 5-7. From a mechanics point of view, this entrapped liquid behaves differently as compared to the free liquid at the grain boundaries. In general, it clearly shows that the traditional reheating microstructure exhibits larger variation in grain morphology as compared to the two-stage reheating microstructure. While this is seen in all the figures, it is especially clear in the micrographs at holding time of 20 min ((b1) in Figs. 5-7). These results demonstrate that the two-stage reheating process provides better microstructure control, which will be a benefit during industrialization.

Fig. 5 shows the semi-solid microstructures obtained after reheating at 843 K for various holding times (15, 20, and 25 min) using both reheating methods. The traditional reheating microstructures are shown in (a1, b1, c1). As can be seen, at a relatively low reheating temperature and short holding time of 15 min (a1), the traditional reheating microstructure presented as irregular and finely-divided dendritic grains with tiny distinct grain boundaries. This micrograph is similar to the initial microstructure, Fig. 1, indicating that although some liquid has melted, there has been only limited grain coarsening. With increased holding time to 20 min, (b1), rosette-like grains have formed. Clearly, the grain boundaries continued to move

and coalesce in order to reduce system energy. Much of the liquid is now also entrapped within the grains. With a further holding time to 25 min, (c1), the grains have further coarsened and a bright third-phase particle, assumed to be blocky Si, has appeared at the grain boundaries or entrapped in solid grains. In comparison to the traditional reheating process, the microstructure obtained from the two-stage process (i.e. first reheat to the liquidus, then cool to 843 K) is significantly different. There appears to be more liquid present, and further the bright phase is not present. With increasing holding time to 20 (b2) and then 25 (c2) min, the solid grains gradually coarsened and also became spherical in shape. At 25 min, it can be observed that a few larger "liquid islands" have formed. These individual grains were relatively coarse in size and irregular in shape; coalescence then played a significant role in the formation of these coarsening grains.

Fig. 6 shows all of the micrographs resulting from using a reheating temperature of 853K. Using the traditional reheating process, the grains are rosette-like in shape after 15 min of heating, (a1), with a small amount of remelted liquid at the grain boundaries. With increasing time to 20 min and then 25 min, (b1, c1), the grains have grown and coalesced together and more of the material has melted. Although the traditional reheating at 853 K required 25 min of hold time, the bright precipitates still cannot be fully melted. This phase, if it remained after thixoforming, could result in component embrittlement. Further, these particles may prevent further coarsening. So it is necessary to melt these precipitates to further improve the morphology of semi-solid microstructure and optimize the thixotropic behavior of resulting parts. Further, as the holding time is extended to 25 min (c1), large drops of liquid are seen to be entrapped inside the coarsening solid grains, and the bright precipitates seem to act as obstacles to grain spheroidization. The liquid is also non-uniformly distributed around the irregular-shaped solid grains.

Two-stage reheating microstructures obtained from first reheating the material to the liquidus and then cooling to 853K are shown in Fig.6 (a2) (b2) (c2). The microstructure resulting from a holding time of 15min, (a2), indicates that the holding time is too short to complete the grain spheroidisation process. There are a few smaller solid grains suspending in the liquid (i.e., suspended grain in structure), which dissolve quickly to reach a new equilibrium condition due to its high curvature. As the holding time is increased to 20min, the solid grains tend to be more globular and uniform in size, demonstrating that the two-stage reheating microstructure, (b2), reaches an equilibrium state, with near-spherical primary phase dispersed uniformly in a liquid matrix. The certain amount of free liquid surrounding at grain boundaries is in favor of a reduction of fluid internal fiction, which is beneficial to the rearrangement and spherical solid grains during processing. The surface tension and boundary energy act as the driving force for the movement and rotation of solid grains. Consequently, this shows that the two-stage reheating process can successfully produce the desirable semi-solid microstructure, as shown in Fig.6 (b2), which is consisted of well-developed completely spheroidal grain and uniformly distributed free liquid at grain boundaries, with only a little amount of liquid entrapped in the solid grains. As the holding time is further increasing to 25 min, (c2), solid grain coarsening to an irregular grain shape is noted. This phenomenon is due to the higher surface energy of the inner crystallites of solid grains, which is contributed to the dissolution of solid grains with

entrapped liquid. For this reason, the low curvature and spherical solid grains is translated into rosette-like solid grains with large curvature [**Error! Bookmark not defined.**].

Fig. 7 shows the comparative semi-solid microstructures with temperature increased to 863K for the two reheating processes. Compared to the traditional microstructures at the lower reheating temperatures, rosette type grain boundaries are visible in the microstructure even after a holding time of 15 min, (a1). At longer holding times, (b1, c1), the traditional reheating microstructures still contain the third-phase precipitation structure, and the solid grains are coarsening, meanwhile a large number of small sized solid grains are present within the liquid at boundaries, which have a great influence on the homogeneous of microstructure. The two-stage microstructures from reheating to 863K are shown in Fig.7 (a2) (b2) (c2). The shape of solid grains is improved (in terms of round-ness) as compared to the traditional microstructure. Further, a lower amount of small suspended grains are evident within the free liquid. Due to the higher temperature, the solid-liquid interfacial energy will be increased, which will enhance the rate of liquid formation. The reheating temperature is too high, diffusion of the solute atoms in the solid-liquid phase is fast as a result of continually growing of liquid phase. So liquid segregation is clearly evident in both traditional and two-stage produced microstructures, with more of the small solid grains suspended in free liquid. It is also obviously observed that liquid segregation and grain coarsening increased as holding time is increased, as shown in Fig.7.

Generally, the coarsening mechanisms of semi-solid microstructure during reheating process are coalescence and Ostwald ripening. The driving force of coarsening mechanism during reheating is the reduction in interfacial energy between the solid and liquid phases [35]. Grain coarsening by coalescence is dominant at short time at a relatively low liquid fraction, while Ostwald ripening plays an increasingly important role with rising of reheating temperature and holding time. At high liquid fractions, the contribution of Ostwald ripening and coalescence lead to a minor entrapped liquid in semi-solid microstructures, as labelled ‘I’ in Figs.5-7. As the reheating temperature increases, both coarsening mechanisms are significantly enhanced as a consequence of boost solid-liquid interface energy and atom diffusion ability. In addition, it can be expected that the liquid entrapped inside of solid grain coarsen as well, with several small adjacent dispersive liquid droplets aggregated into one large central pool. Simultaneously, a local zone of some of particles melted to form irregular solid grain shape, as shown in Figs.5-7.

3.2 Quantitative metallography

To quantify the differences between the traditional and two-stage reheating microstructures, the fraction of entrapped liquid, grain perimeter and area were measured using the Image Pro Plus software. From this data, the equivalent diameter and roundness of the solid grains were calculated using Eq. (1) and Eq. (2), while the coarsening rate constant was estimated from Eq. (3). The fraction entrapped liquid, which represents the possibility of causing defect, was also recorded. Ostwald ripening and coalescence both contribute to the coarsening of grains in a competitive state. These two mechanisms have opposite effects on entrapped liquid, Ostwald ripening leads to a loss of entrapped liquid and coalescence leads to liquid entrapment [36].

The equivalent diameter, roundness and coarsening rate constant of solid grains with variations of holding time at 853K were analyzed by comparing the traditional and the new two-stage reheating processes produced microstructures. The results of this analysis are shown in Fig. 8.

Overall, it is observed that the equivalent diameter (D_{eq}) is smaller, the roundness of grain shape (*F*) is closer to 1, the coarsening rate (*K*) is lower and there is less entrapped liquid ($f_{l,en}$) in the two-stage reheating microstructure as compared to the traditional process. Thus, quantitative metallographic results have demonstrated that the proposed two-stage method can obtain better semi-solid microstructural morphologies.

The statistical analysis of the quantitative metallography is shown in Tables 3 and 4. As can be seen, all p-values of the Wilcox tests for microstructure morphology parameters (*F*, D_{eq}, $f_{l,en}$ and *K*) are below the significance level of 0.05, namely the null hypothesis is refused and their mean value are not equal to each other. This provides strong evidence that the microstructure morphology parameters (*F*, D_{eq}, $f_{l,en}$ and *K*) obtained from two-stage reheating process are markedly different from those obtained from the traditional reheating processes ($p<0.05$). In terms of thixoforming, the semi-solid microstructure is significantly improved by two-stage reheating process.

Table 3 The p-values from the Wilcox tests (α=0.05) for the microstructure morphology parameters measured from the traditional and two-stage reheating samples prepared with the same temperatures and holding periods.

Wilcox tests(p-value) Reheating parameters	*F**	*F*	D_{eq}	L_{en}
843K, 15min	< 2.2e-16	< 2.2e-16	< 2.2e-16	0.02949
843K, 20min	4.425e-15	4.425e-15	0.04114	< 2.2e-16
843K, 25min	9.777e-09	9.777e-09	9.841e-05	4.205e-07
853K, 15min	< 2.2e-16	< 2.2e-16	0.008855	< 2.2e-16
853K, 20min	6.657e-13	6.657e-13	0.01019	5.717e-05
853K, 25min	1.919e-13	1.919e-13	0.00218	1.014e-09
863K, 15min	< 2.2e-16	< 2.2e-16	0.001837	< 2.2e-16
863K, 20min	< 2.2e-16	< 2.2e-16	0.002149	0.0002948
863K, 25min	< 2.2e-16	< 2.2e-16	1.648e-13	0.001116

Table 4 The p-Value of Wilcox tests (α=0.05) for coarsening rate constant during two different reheating processes

Wilcox tests(p-value) Reheating temperature(K)	$K_{20.15}$	$k_{25.20}$
843	< 2.2e-16	< 2.2e-16
853	< 2.2e-16	< 2.2e-16
863	< 2.2e-16	< 2.2e-16

Overall, based on quantitative metallography and statistical analysis results, it can be observed that there is a considerable difference in microstructure between images, and thus considerable

grain evolution is occurring as a function of reheating temperature and reheating time. It was found that it is difficult to produce the well-behaved spherical microstructure by the traditional reheating process for Al-Si casting aluminum alloy. However, the two-stage reheating microstructures exhibited relatively spheroidal and homogeneously distributed grains with a liquid phase that was located along the grain boundaries, and without the bright third-phase precipitates. The two-stage reheating process developed in this work consists of two successive stages to ensure the formation of near-spherical primary solid grains with uniform surrounding liquid phase. The heating to nearly the liquidus as a first stage is crucial to ensure the fully melting of third-phase precipitates at the grain boundaries and to allow for the further optimization of the semi-solid microstructure morphology of Al-Si casting aluminum alloy.

4. Conclusions

The thixoforming process offers an alternative production route for structural components used in the automobile and aerospace industries. The experimental results presented in this work provide some guidance in allowing this process to be applied to industrial Al-Si casting alloys. The main conclusions are noted below.

(1) A two-stage reheating process offers significant advantages over the traditional reheating process in creating feedstock for thixoforming from industrial Al-Si casting alloys.

(2) The first stage of the two-stage process, heating to the liquidus temperature, ensures the complete melting of the third-phase precipitates, and assists in producing small solid grains, and uniformly distributed and near-spherical grains with the liquid phase dispersed uniformly around the solid.

(3) The second stage allows for some grain coarsening, and for the creation of near-spherical grains. Statistically, the equivalent diameter of grains produced using the two-stage process were finer and much more spherical as compared to the traditional process.

(4) The coarsening and entrapped liquid contents were measured and noted as also being lower for the two-stage reheating microstructure compared to that of traditional process.

Acknowledgements

This work is funded by the National Natural Science Foundation Project of China (51374109). The authors would like to thank to Analyst Shou Peng Xie in Shanghai Lian He Credit Information Service Co., Ltd for his assistance in statistical analysis and helpful discussions.

5. Reference

[1] K.N. Campo, C.T.W. Proni, and E.J. Zoqui: Influence of the processing route on the microstructure of aluminum alloy A356 for thixoforming. Mater. Charact. 85, 26 (2013).

[2] Q. Chen, Z. Zhao, G. Chen, and B. Wang: Effect of accumulative plastic deformation on generation of spheroidal structure, thixoformability and mechanical properties of large-size AM60 magnesium alloy. J. Alloys Compd. 632, 190 (2015).

[3] G. Chen, Q. Chen, B. Wang and Z.-m. Du: Microstructure evolution and tensile mechanical properties of thixoformed high performance Al-Zn-Mg-Cu alloy. Met. Mater. Int. 21(5), 897 (2015).

[4] Z. Chen, T. Wang, L. Gao, H. Fu, and T. Li: Grain refinement and tensile properties improvement of aluminum foundry alloys by inoculation with Al–B master alloy. Mater. Sci. Eng. A. 553, 32 (2012).

[5] C. Ai, X. Zhao, L. Liu, H. Zhang, Y. Ru, Y. Pei, J. Zhou, S. Li, and S. Gong: Influence of withdrawal rate on last stage solidification path of a Mo-rich Ni 3 Al based single crystal superalloy. J. Alloys Compd. 623, 362 (2015).

[6] K. Huang, N. Wang, Y. Li, and K. Marthinsen: The influence of microchemistry on the softening behaviour of two cold-rolled Al–Mn–Fe–Si alloys. Mater. Sci. Eng. A. 601, 86 (2014).

[7] S. Jia, D. Zhang, and L. Nastac: Experimental and numerical analysis of the 6061-based nanocomposites fabricated via ultrasonic processing. J. Mater. Eng. Perform. 24(6), 2225 (2015).

[8] C. Ai, S. Li, H. Zhang, L. Liu, Y. Ma, Y. Pei, and S. Gong: Effect of withdrawal rate on microstructure and lattice misfit of a Ni 3 Al based single crystal superalloy. J. Alloys Compd. 592, 164 (2014).

[9] K. Du, Q. Zhu, D. Li, and F. Zhang: Study of formation mechanism of incipient melting in thixo-cast Al–Si–Cu–Mg alloys. Mater. Charact. 106, 134 (2015).

[10] S.Z. Shang, J.J. Wang, G.M. Lu, and X.L. Tang: Study on the semi-solid thixo-diecasting process of aluminum alloys and die design, in Solid State Phenomena, (192, Trans Tech Publ, City, 2013), pp. 460.

[11] Q. Chen, G. Chen, L. Han, N. Hu, F. Han, Z. Zhao, X. Xia, and Y. Wan: Microstructure evolution of SiC p/ZM6 (Mg–Nd–Zn) magnesium matrix composite in the semi-solid state. J. Alloys Compd. 656, 67 (2016).

[12] J.J. Wang, G.M. Lu, and J.G. Yu: Numerical Analysis of Semi-Solid Die-Casting Automobile Part Based on the Thermo-Visco-Plastic Constitutive Relation, in Advanced Materials Research, (1096, Trans Tech Publ, City, 2015), pp. 268.

[13] X. Zhu, W. Jiang, M. Li, H. Qiao, Y. Wu, J. Qin, and X. Liu: The Effect of Mg Adding Order on the Liquid Structure and Solidified Microstructure of the Al-Si-Mg-P Alloy: An Experiment and ab Initio Study. Metal. 5(1), 40 (2014).

[14] K. Huang, O. Engler, Y. Li, and K. Marthinsen: Evolution in microstructure and properties during non-isothermal annealing of a cold-rolled Al–Mn–Fe–Si alloy with different microchemistry states. Mater. Sci. Eng. A. 628, 216 (2015).

[15] J. Wang, S. Shang, G. Lu, and J. Yu: Viscosity estimation of semi-solid alloys based on thermal simulation compression tests. Int. J. Mater. Res. 104(3), 255 (2013).

[16] S. Zabler, A. Ershov, A. Rack, F. Garcia-Moreno, T. Baumbach, and J. Banhart: Particle and liquid motion in semi-solid aluminium alloys: A quantitative in situ microradioscopy study. Acta Mater. 61(4), 1244 (2013).

[17] D. Brabazon, D. Browne, and A. Carr: Mechanical stir casting of aluminium alloys from the mushy state: process, microstructure and mechanical properties. Mater. Sci. Eng. A. 326(2), 370 (2002).

[18] E. Tzimas, and A. Zavaliangos: Mechanical behavior of alloys with equiaxed microstructure in the semisolid state at high solid content. Acta Mater. 47(2), 517 (1999).

[19] Y. Meng, S. Sugiyama, and J. Yanagimoto: Microstructural evolution during partial melting and semisolid forming behaviors of two hot-rolled Cr–V–Mo tool steels. J. Mater. Process. Technol. 225, 203 (2015).

[20] S. Jia, and L. Nastac: The influence of ultrasonic stirring on the solidification microstructure and mechanical properties of A356 alloy. Chem. Mater. Eng. 1(3), 69 (2013).

[21] L. Zhu, and H.Y. Sohn: Growth of 2M-wollastonite polycrystals by a partial melting and recrystallization process for the preparation of high-aspect-ratio particles. J. Ceram. Sci. Technol. 3(4), 169 (2012).

[22] M. Moradi, M. Nili-Ahmadabadi, B. Poorganji, B. Heidarian, and T. Furuhara: EBSD and DTA characterization of A356 alloy deformed by ECAP during reheating and partial re-melting. Metall. Mater. Trans. A 45(3), 1540 (2014).

[23] J. Wang, A. Phillion, and G. Lu: Development of a visco-plastic constitutive modeling for thixoforming of AA6061 in semi-solid state. J. Alloys Compd. 609, 290 (2014).

[24] G. Padhy, C. Wu, S. Gao, and L. Shi: Local microstructure evolution in Al 6061-T6 friction stir weld nugget enhanced by ultrasonic vibration. Mater. Des. 92, 710 (2016).

[25] G. Chen, Q. Chen, J. Qin, and Z.-m. Du: Effect of compound loading on microstructures and mechanical properties of 7075 aluminum alloy after severe thixoformation. J. Mater. Process. Technol. 229, 467 (2016).

[26] Y. Birol: Comparison of thixoformability of AA6082 reheated from the as-cast and extruded states. J. Alloys Compd. 461(1), 132 (2008).

[27] J. Wang, D. Brabazon, A. Phillion, and G. Lu: An innovative two-stage reheating process for wrought aluminum alloy during thixoforming. Metall. Mater. Trans. A 46(9), 4191 (2015).

[28] A. Kearney: Properties of cast aluminum alloys ASM International, Metals Handbook, Tenth Edition. 2, 152 (1990).

[29] D. Liu, H.V. Atkinson, and H. Jones: Thermodynamic prediction of thixoformability in alloys based on the Al–Si–Cu and Al–Si–Cu–Mg systems. Acta Mater. 53(14), 3807 (2005).

[30] A. Abedi, M. Shahmiri, B.A. Esgandari, and B. Nami: Microstructural Evolution during Partial Remelting of Al–Si Alloys Containing Different Amounts of Magnesium. J. Mater. Sci. Tech. 29(10), 971 (2013).

[31] M.S. Salleh, M.Z. Omar, and J. Syarif: The effects of Mg addition on the microstructure and mechanical properties of thixoformed Al–5% Si–Cu alloys. J. Alloys Compd. 621, 121 (2015).

[32] S. Shankar, Y.W. Riddle, and M.M. Makhlouf: Eutectic solidification of aluminum-silicon alloys. Metall. Mater. Trans. A 35(9), 3038 (2004).

[33] A. Bolouri, M. Shahmiri, and C.G. Kang: Coarsening of equiaxed microstructure in the semisolid state of aluminum 7075 alloy through SIMA processing. J. Mater. Sci. 47(8), 3544 (2012).

[34] P. Dalgaard: Introductory statistics with R (Springer Science & Business Media, City, 2008), pp. 95,107.

[35] Z. Wang, Z. Ji, M. Hu, and H. Xu, Evolution of the semi-solid microstructure of ADC12 alloy in a modified SIMA process, Mater. Charact. 62(2011) 925-930.

[36] Babaghorbani P, Salarfar S, Nili-Ahmadabadi M. Kinetics of coarsening and solid sphericity during reheating of ductile iron and Al alloys. In Solid State Phenomena 2006 Oct 7 (Vol. 116, pp. 205-208).

This article has been published in the Journal of Materials Research. The final publication is available at Cambridge via https://doi.org/10.1557/jmr.2016.163 .

Figure captions

Fig.1 Initial dendritic microstructure of the 356.0v casting alloy obtained by vertical electromagnetic continuous casting

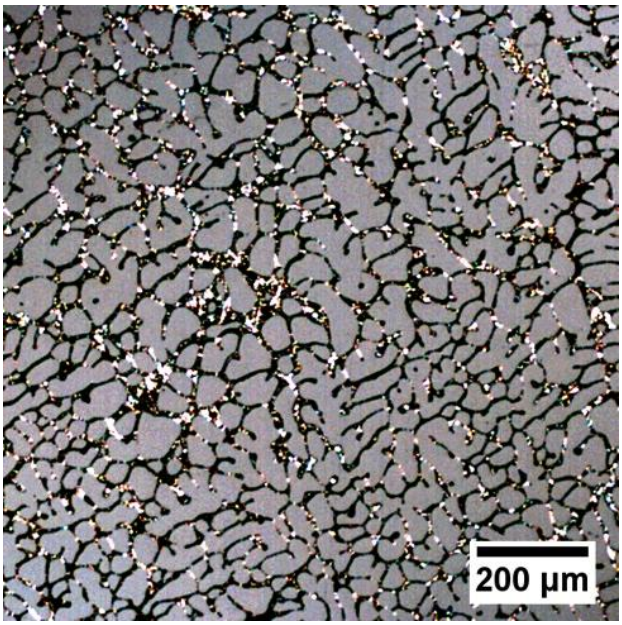

Fig.2 Differential thermal analysis curve of 356.0v during heating process at a rate of 10K/min

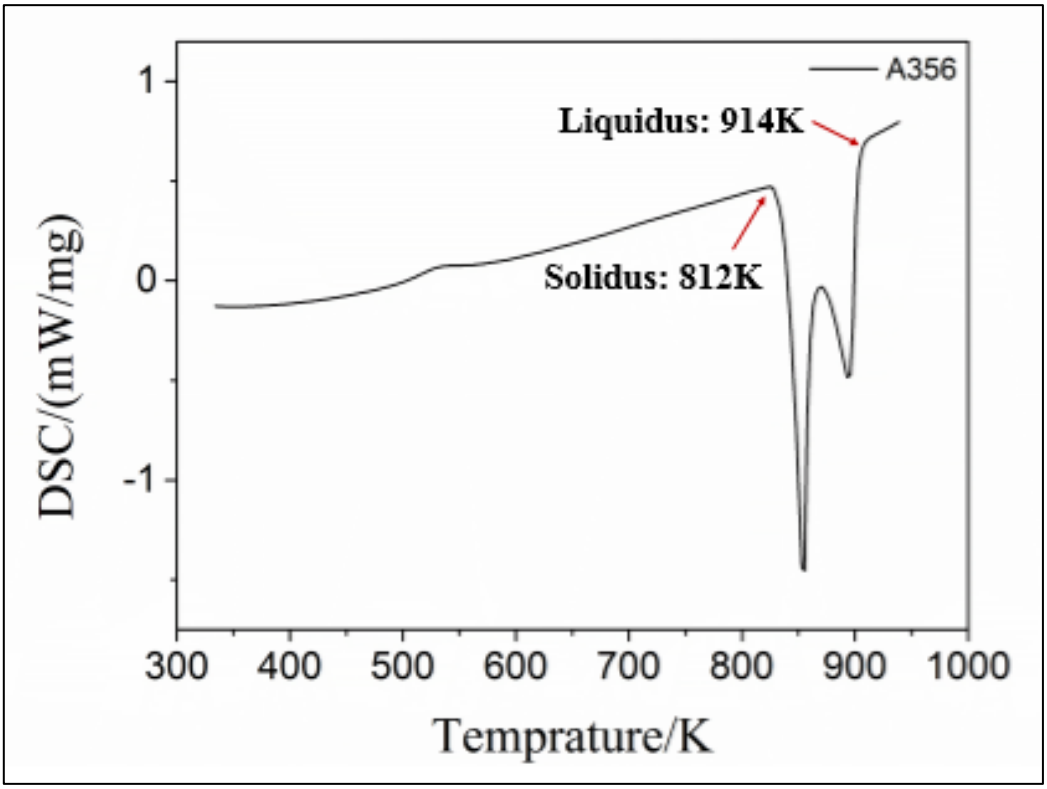

Fig. 3 Change in liquid fraction with temperature of 356.0v casting alloy derived from the recorded DSC curve at a heating rate of 10K/min

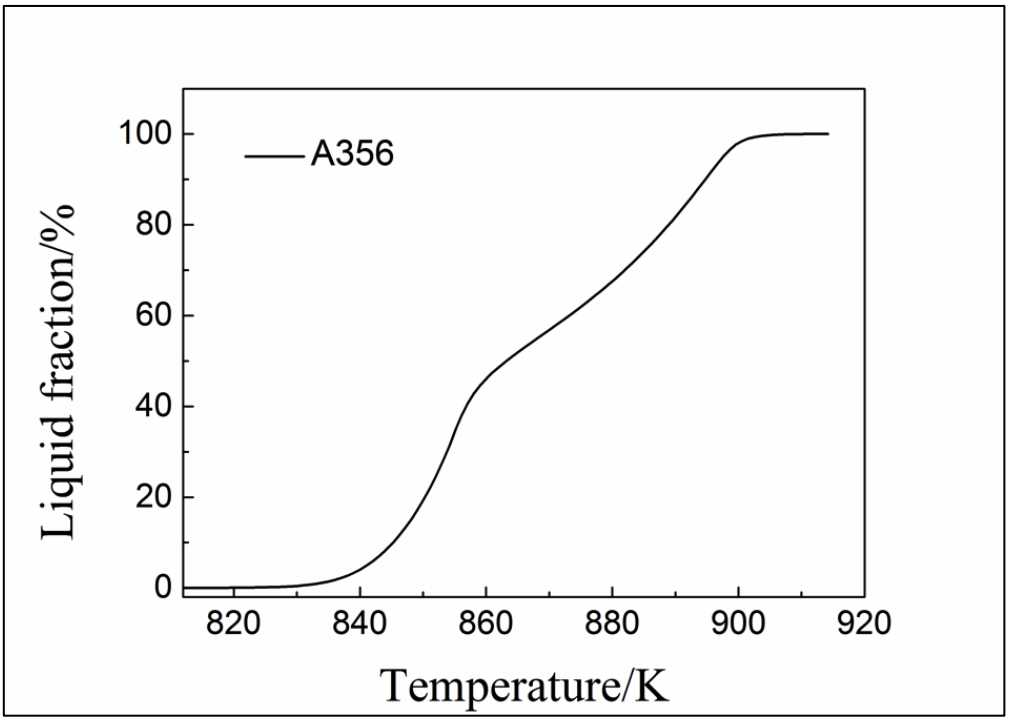

Fig. 4 reheating temperatures vs times used for investigation of the two-step reheating process for Al-Si casting alloy

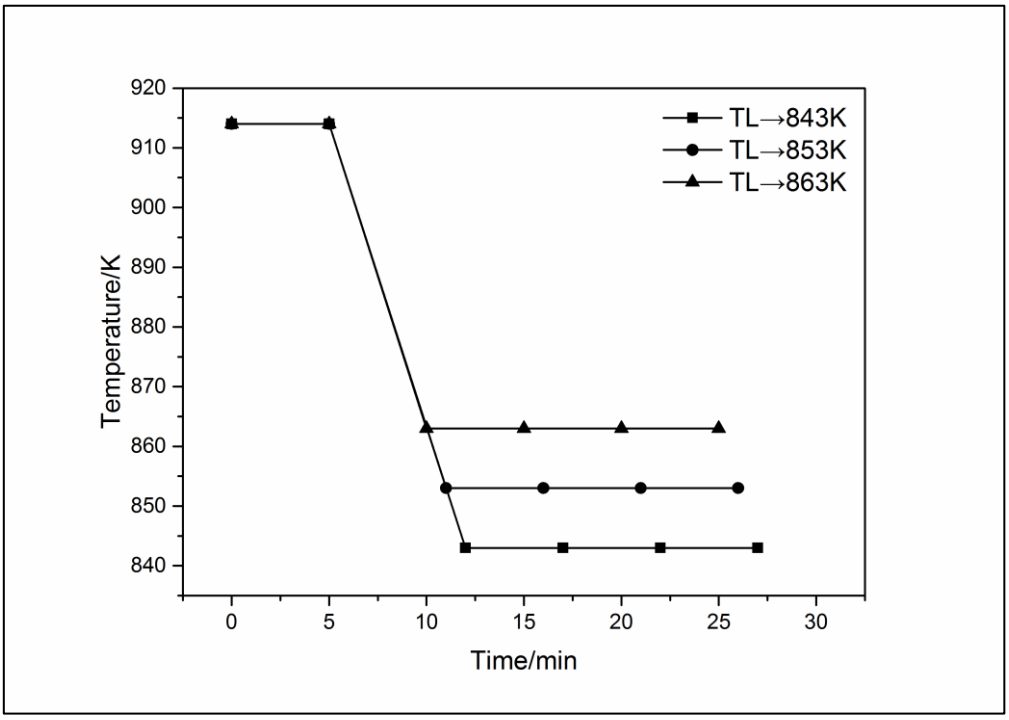

Fig. 5 Microstructures of 356.0v obtained from traditional (a1, b1, c1) and two-stage (a2, b2, c2) reheating process prepared at 843K with different soaking periods: (a) 15 min; (b) 20 min; (c) 25 min

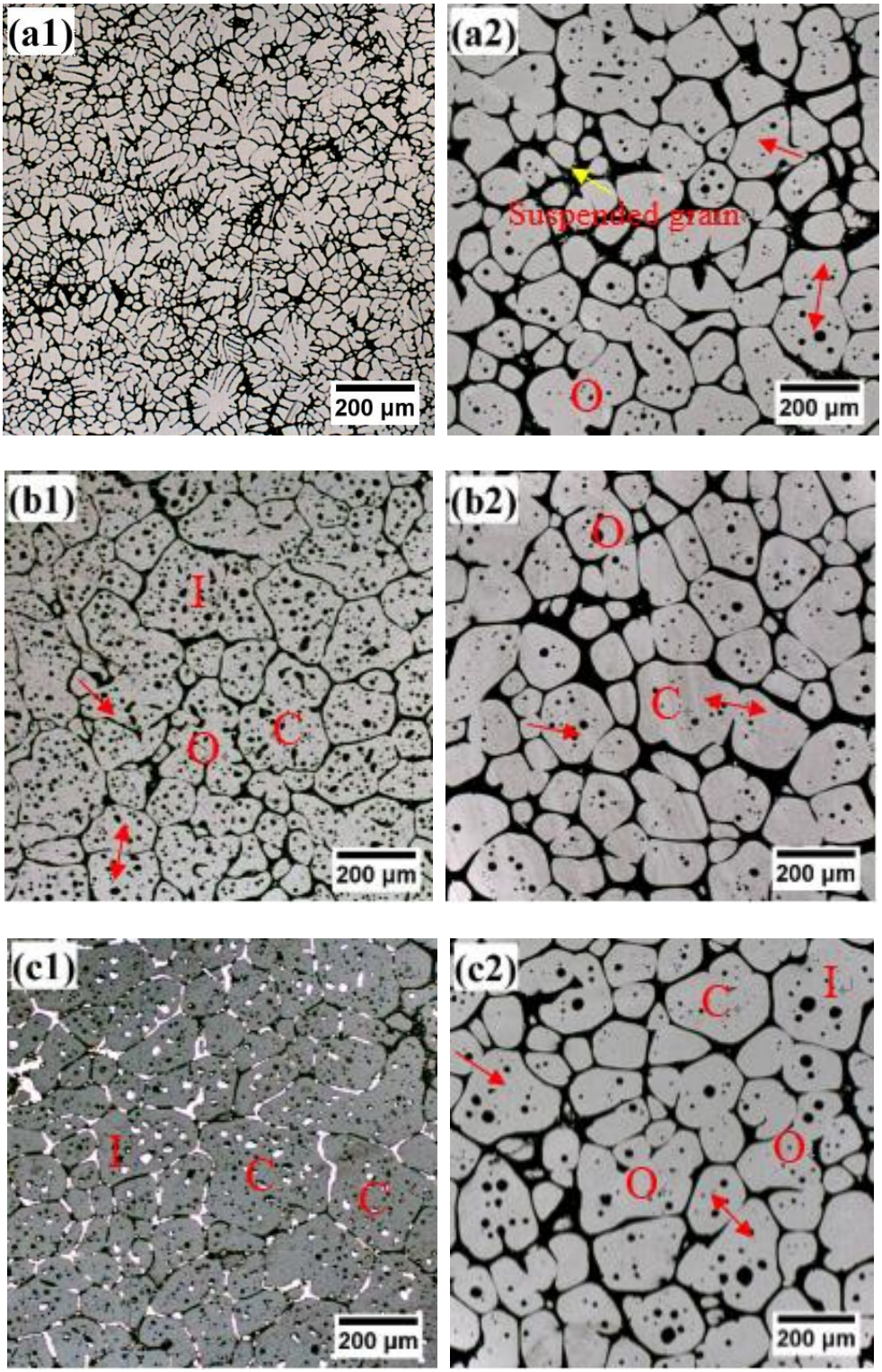

Fig. 6 Microstructures of 356.0v obtained from traditional (a1, b1, c1) and two-stage (a2, b2, c2) reheating process prepared at 853K and with different soaking periods: (a) 15 min; (b) 20 min; (c) 25 min

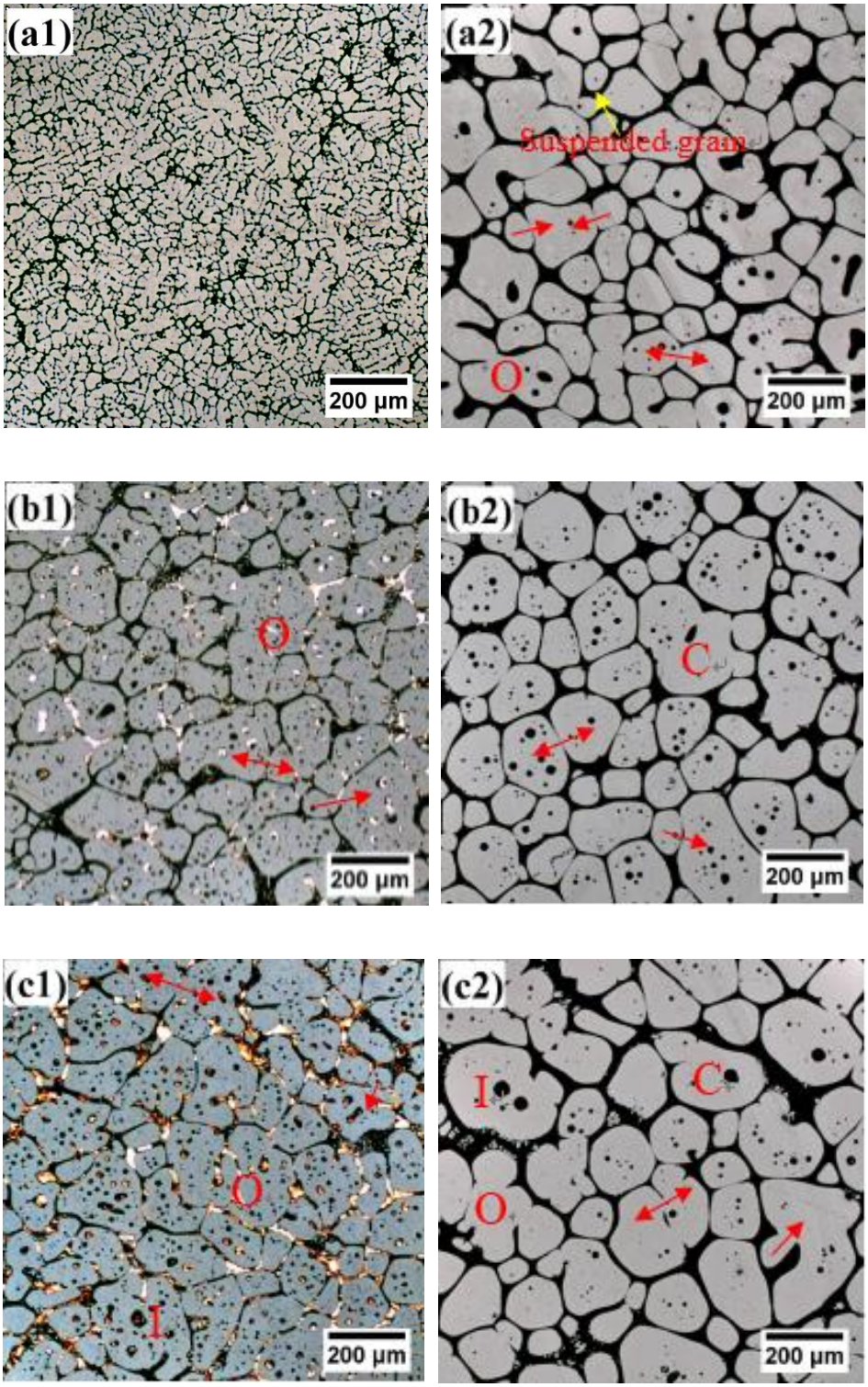

Fig. 7 Microstructures of 356.0v obtained from traditional (a1, b1, c1) and two-stage (a2, b2, c2) reheating process prepared at 863K with different soaking periods: (a) 15 min; (b) 20 min; (c) 25 min

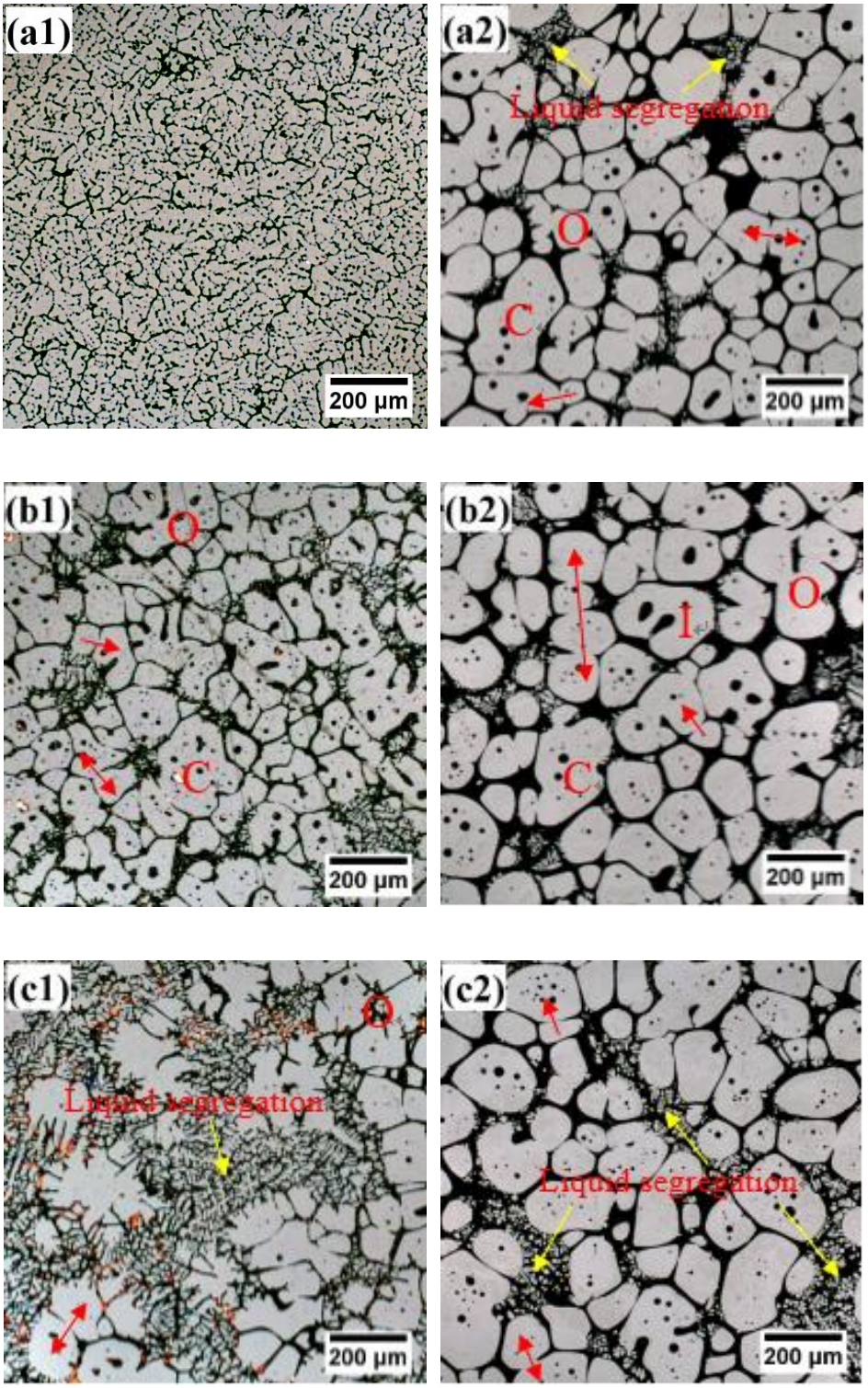

Fig. 8 Dependence of (a) equivalent diameter, roundness, (b) coarsening rate constant and fraction entrapped liquid on holding time at a temperature of 853K from the traditional and two-stage reheating process for 356.0v casting alloy

a)

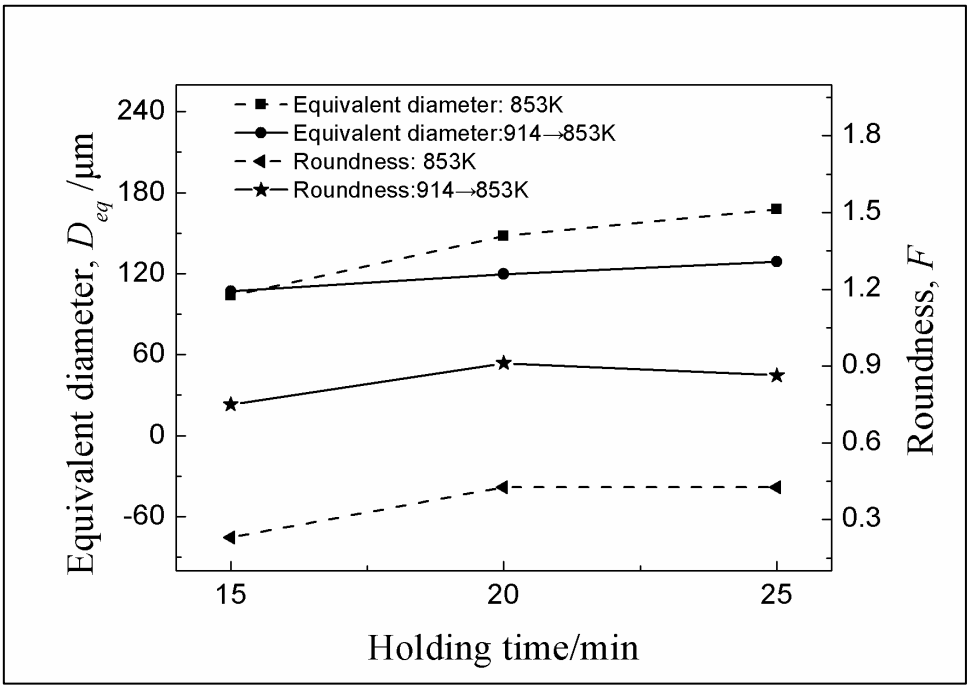

b)